MICROSEISMS AT PALISADES: 1. SOURCE LOCATION AND PROPAGATION

D. H. Rind and W. L. Donn

Lamont-Doherty Geological Observatory of Columbia University, Palisades, N.Y.10964

Abstract. Microseisms recorded at Palisades, New York are investigated as to the source location, propagation paths, and relation to ocean wave heights. The source location is estimated from analysis of the incoming wave ground motion by using an analog correlator to compute the direction of propagation and then tracing this ray to a suspected meteorological-oceanographic source. The propagation path of Rayleigh waves approaching Palisades is determined, taking into account the geological and bathymetric structure of the western North Atlantic, and the resulting ray diagram is used to explain some of the source frequency observations. The amplitude of observed microseisms is shown to be a function of the ocean wave heights in the suspected generating region and is a result of both refraction effects as well as apparently 'off the continental shelf' source locations. The principal conclusions are as follows: (1) The majority of sources producing microseisms at Palisades occur either in regions on the continental shelf to the east and northeast or off the continental shelf to the southeast, although the latter produce weaker signals. (2) The relative lack of sources in the region along the southeast coast on the continental shelf appears to be due to refraction effects. (3) The closer the origin is to the east or northeast on the continental shelf, the higher are the microseisms produced by given ocean waves although the relationship has too much scatter to allow ocean wave heights to be determined with great enough certainty from microseism observations.

Introduction

Microseisms have been observed and investigated for more than 100 years with increasing sophistication. In the last 15 years, large-scale arrays in Montana and Norway (e.g., Rygg et al., 1969; Haubrich and McCamy, 1969) have provided detailed analyses of observations. Ocean bottom and midwater seismographs (e.g., Latham and Sutton, 1966; Bradner et al., 1970) have produced data from previously inaccessible regions. Yet many questions remain unanswered, and there continue to be disparities between observations. Explanations that were offered in the past have now been investigated and found unsatisfactory. For example, are microseisms which are recorded on land generated mostly on the continental shelf, with deep-sea storms having little effect? Observations tend to favor this hypothesis (e.g., Donn, 1957; Haubrich and McCamy, 1969), although not unanimously (e.g., Iyer, 1958). If so, is this the effect of generation or propagation? The midwater and ocean bottom seismographs noted above indicate that generation off the continental shelf does occur. As a propagation effect, is it because of refraction (e.g., Donn, 1954; Haubrich et al., 1963), energy transfer out of the fundamental mode (e.g., McGarr, 1969) or damping traveling along the ocean bottom (Monakhov, 1962)? What is the relationship between the ocean wave source and resulting microseisms? What is the wave type involved in microseisms--Rayleigh or Love--and if there is Love wave energy, how is it formed?

In the following series of articles we will resurrect several of these long-standing problems. In this paper we will address the question of generating region (offshore versus onshore) by noting the probable location of the oceanographic sources of microseisms observed at Palisades. We will investigate the effect of refraction by deriving the propagation paths for 5-s microseisms on the basis of geology and bathymetry for the western North Atlantic. We will see how the microseism amplitude varies for ocean wave sources in different regions by comparing the observed ocean wave amplitude in the suspected source regions with the microseisms recorded at Palisades. In the following articles we will discuss the Rayleigh and Love wave characteristics of microseisms at Palisades and also provide results of a long-term statistical comparison between microseisms and simultaneously recorded microbaroms-infrasound of the same frequency believed to be generated concurrently with microseisms. This study represents the first general compilation of observations of microseisms for a station on the east coast of North America.

Instrumentation and Procedure

At Palisades, New York (41°00'25"W), there is maintained a three-component seismograph of three closely matched pendulums with free periods of about 15 s coupled through an electromagnetic transducer to Benioff model 6000 galvanometers that have a free period of 75 s. The observations are displayed in the normal manner on rotating drums. Signal is recorded on analog tape from a

Paper number 8B0274.
0148-0227/78/078B-0274$01.00

parallel system of seismographs. The tape data were analyzed with the use of the Saicor SAI-42 correlation and probability analyzer as well as the Saicor SAI-51 real time spectrum analyzer-digital integrator.

The procedure adopted was as follows: approximately 800 hours of data, collected from 1968-1971, were analyzed to determine the amplitude, frequency, and direction of propagation. The amplitude was obtained from the well-calibrated visual photographic charts as well as the square root of the value at zero time lag of the autocorrelation of the tape signal. The first method involves measuring a number of waves and estimating the mean; the second gives the mean amplitude of all of the waves for each hour (720 waves of approximately 5-s period) and is more exact. Both were employed, however, to check for spurious amplitude changes of the tape system, which occasionally occur. The frequency-amplitude spectrum for each hour was displayed on an oscilloscope and copied directly.

To determine the direction of propagation of microseisms from a single-station three-component seismograph, we employed the method apparently first proposed by Leet in 1929 (Ikegami and Kishinouye, 1951) of computing the direction of arrival by assuming that the microseisms contained a significant proportion of Rayleigh wave energy which would have retrograde elliptical particle motion for the local ground structure (0.25 km diabase overlying 0.25 km of sediments (shales and sandstones) above a thick base of crystalline rock). The NS component was correlated with the Z component for each hour of data by using the SAI-42 correlation, with the amplitude of the correlation function noted, as well as the lead or lag time. The correlation procedure was then repeated for the EW and Z component. For Rayleigh (R) waves the horizontal components should be out of phase with the vertical and in phase with each other; the absolute values of the time delay between each horizontal component and the vertical should be equal. The Rayleigh wave characteristics of the signal will be discussed more fully in the next paper, but suffice it to say that these expected effects were observed more than 90% of the time, verifying the assumption of considerable Rayleigh wave energy. The orientation of the horizontal particle motion ellipse is obtained by

$$\theta = \tan^{-1} \frac{A(EW-Z)}{A(NS-Z)}$$

where θ is the azimuth angle measured from the north, and A is the amplitude of the covariance function between the horizontal and the vertical component at a delay time corresponding to the peak correlation. As the delay time was almost always the same for each horizontal vertical correlation and the horizontal components were being correlated with the same (vertical) signal, the ratio indicates the relative strengths of the two horizontal components which are associated with the vertical component. This removes any misleading effect due to Love waves which would not correlate with any vertical component. The result is also obtained from

$$\theta = \tan^{-1} \frac{C(EW-Z)}{C(NS-Z)}$$

where C is the root coherence of the components. The only difference between the two formulas is that the root coherence is obtained by, for example,

$$C(EW-Z) = \frac{A(EW-Z)}{(EW)^{\frac{1}{2}}(Z)^{\frac{1}{2}}}$$

the terms in the denominator representing the square root of the autocorrelation at zero time delay for each component. Any spurious amplitude changes affecting only one component are removed by the normalization (affecting both numerator and denominator), and thus the use of coherence provides better accuracy.

What is the resolution of this technique? An investigation between directions determined from particle motions and directions from a **tripartite** array of seismometers showed that when Rayleigh wave energy was considered, the two directions of approach were 'quite in agreement' (Ikegami and Kishinouye, 1951) (from the examples shown, less than 10° deviation is apparent). The reliability of the tripartite method was judged by comparison between two tripartite arrays and shown to be within 5° of azimuth (Ikegami, 1962). Thus the resolution of the particle motion method seems adequate for the purposes described here, especially considering that our procedure utilizes far more data than the hand-plotted construction of particle ellipses from individual waves, which has been usual in the past for single-station analysis. However, a meaningful answer is obtained by averaging signals of 5-s period for 1 hour only if the signal is ergodic. This assumption has been shown to be valid by Haubrich (1965) and Rygg et al. (1969), and it agrees with our observations insofar as the directions calculated for varying time intervals up to an hour are in general agreement with each other.

Observations Related to Source Locations

The direction of propagation of the microseisms was thus determined by calculating the azimuth of the major axis of the elliptical particle motion projected to the horizontal and

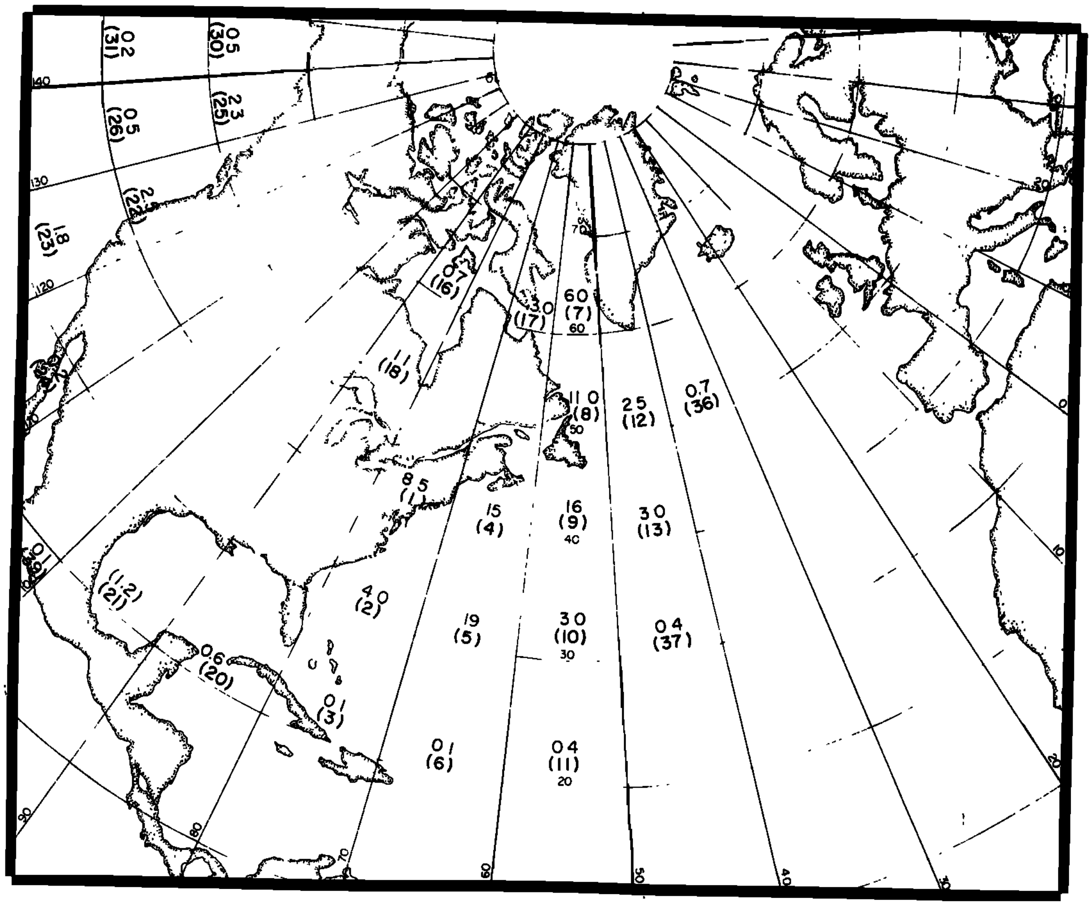

Fig. 1. Frequency (in percent of 800 hours) of microseism sources in estimated source locations from 1968 to 1971. 10^{o}x10^{o} regions are identified by numbers in parentheses.

reconstructing the retrograde particle motion by noting the lag or lead character of the correlation between the horizontal and the vertical component. The suspected sources of microseisms are interfering ocean waves of relatively large amplitude and a period of about 2 times that of the resulting seismic signal. To estimate the source location, a line was drawn from the station in the direction of the incoming signal to the nearest region of marine storminess and/or high ocean waves. 'Marine storminess' included all synoptic-scale systems such as low-pressure centers, cold, warm, occluded, and stationary fronts, or simply the wake of rapidly moving low-pressure systems, all regions where interfering waves resulting from horizontal wind shear could be expected. High ocean waves were all ocean waves of 10 feet (3 m) or greater, usually coinciding with one of the above meteorological features but sometimes remaining after the synoptic feature has moved away or dissipated. The location of weather systems was determined from appropriate northern hemisphere and United States weather maps for the appropriate times; charts of ocean wave heights for each of the appropriate days were prepared by the U.S. Navy Fleet Weather Central. In addition, the frequency spectrum of the recorded microseism signal was determined, as was noted earlier, and the necessary period of the generating ocean waves calculated (theoretically equal to 2 times the period of the observed microseisms). The required ocean wave periods ranged from 6 to 20 s. Ocean wave periods for the appropriate days for locations in the North Pacific and North Atlantic were also obtained from the Navy Fleet Weather Center, and when they were compared with the measured source periods, they helped to define further the source location as well as to distinguish between closer and further potential sources. This study must of necessity be considerably subjective; with only one receiving array we cannot know where the source is, only in what direction it lies. Nevertheless, certain criteria can be heeded: does the signal amplitude weaken when the estimated source weakens or moves away; does the azimuth of the signal change appropriately as the suspected source moves and remain stationary when the source is stationary; do certain repeating conditions continually act as potential sources? All of these factors have been considered as closely as possible.

In Figure 1 the percentage of deduced

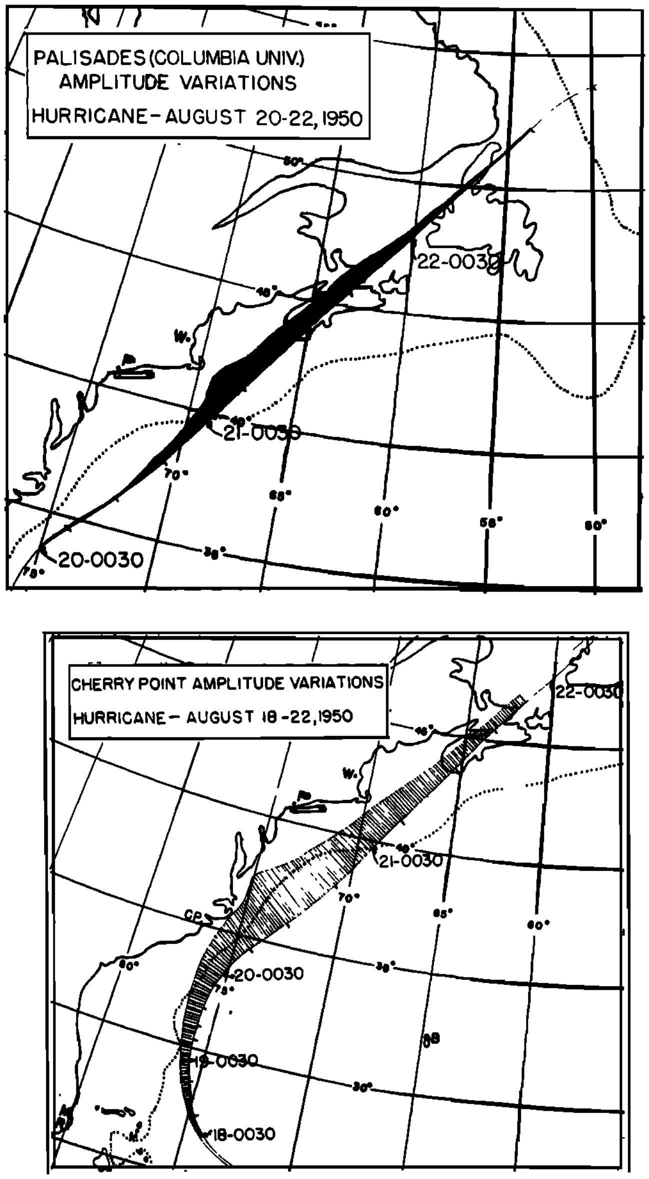

Fig. 2. (a) Relative amplitude received at Palisades (P) (arbitrary units) when hurricane of August 18-22, 1950, was in various locations is indicated by height of the curve above the storm tract. (b) Same as Figure 2a except at Cherry Point (CP).

source locations for different 10^{o}x10^{o}grid spacings is presented. In a grid of this size, slight errors in estimating source locations are unimportant, and the estimated resolution noted above is sufficient to locate a source within a given grid. For ease in referral, each grid spacing is provided with an identifying number (the numbers in parentheses in the figure).

The results indicate that the signal is often received from locations near shore, on the continental shelf. Fifty percent of the time the observed microseisms at Palisades are estimated to come from the area that includes regions 1, 4, 8, and 9. Regions to the north and north-northeast have a larger number of sources than regions to the south; regions 2, and 3, on the continental shelf, account for less than 5% of the observed signal. In contrast, region 5, to the southeast and off the continental shelf, accounts for nearly 20% of the times of signal observation, although signal from this region is generally weak.

For other regions it is generally true that the farther the grid location is from Palisades, the less it accounts for observed microseisms. West Coast and Gulf Coast sources are occasionally perceived but are usually masked by the much closer Atlantic Ocean sources.

The two major results of this survey are that sources off the continental shelf appear (as does region 5) to produce observable, although weak, microseisms at Palisades, while sources on the continental shelf to the south rarely do so. The latter result has been noted previously. Donn (1957) showed that coastal stations north of Cape Hatteras record only weak microseisms from storms to the south. Microseisms from the hurricane of August 20-22, 1950, show a rather typical amplitude pattern. Figure 2a shows relative microseism amplitude at Palisades (P) plotted along the track of the center of the storm. Microseisms from the south when the hurricane was below 37°N have negligible amplitude. The latter rose noticeably when the storm moved to the southeast of the station (P). As a control, Figure 2B shows that microseisms were recorded with high amplitude at Cherry Point (CP) from the storm when it was well below the 37° cutoff for Palisades. Although it has been shown by Donn (1957) that microseism sources must be over the continental shelf for significant microseisms to be recorded in eastern North America, this is not a factor in the present case, as much of the storm was over the shelf, as can be seen by reference to the dotted 1000-fathom (1800 m) bathymetric contour. A factor other than location of the source must be involved.

Propagation Paths

It has long been speculated that effects such as this may, in part, be the result of refraction. Rayleigh wave velocity decreases with an increase of low-velocity sediments and also with greater water depths. The resulting velocity variation results in curved ray paths.

To investigate this effect, refraction diagrams for microseisms of 5-s period were constructed on the basis of both geologic and bathymetric variations of the propagation medium off the east coast of North America. The bathymetric data was obtained from maps of the North

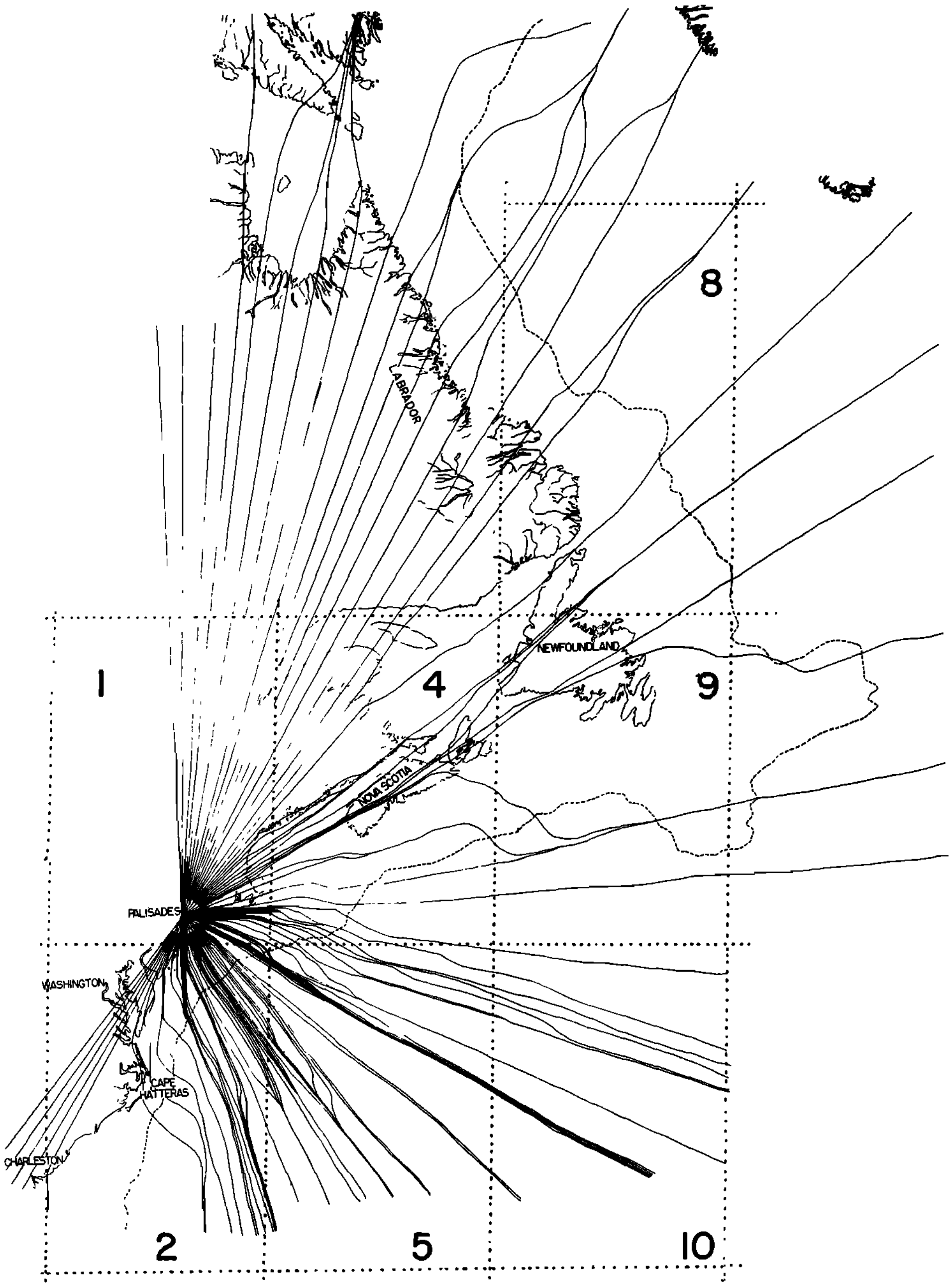

Fig. 3. Refraction diagram for microseisms of 5-s period approaching Palisades, based on geologic and bathymetric profiles of the western North Atlantic. Grid refers to presentation in Figure 1.

Atlantic Ocean-Northwestern and Southwestern Sheets (1967) enlarged to a scale of 1:9,000,000. The geologic data depicting the vertical and horizontal cross sections of the western North Atlantic ocean floor were obtained from Heezen et al. (1959) for general cross sections and from Houtz and Ewing (1963), Drake et al. (1963), J. Ewing and M. Ewing (1959) , Fenwick et al. (1968), Sheridan and Drake (1968), Nafe and Drake (1969), and Le Pichon et al.(1971) for specific regions.

From the different geologic and bathymetric observations it was necessary to construct Rayleigh wave velocities. To do this we utilized the computer model developed by Kutschale (1970, 1971), into which is input compressional velocity, shear velocity, and density as a function of depth, from which is received, among other things, Rayleigh wave velocity as a function of period. We used the results for 5-s period, the mean for microseisms recorded at Palisades. In addition to the references noted above for the geologic data, special attention was paid to the variation of the input parameters with depth on the continental shelf in regions of thick sedimentation under shallow water. The compressional velocities along the U.S. coast were determined for a given depth, after Sheridan et al. (1966), by

$V_{comp} = 6.00(1-0.72e^{-0.5z})$ for terrigenous

elastic sediments north of Cape Hatteras and by $V_{comp} = 6.00(1-0.72e^{-1.2z})$ for high-carbonate sediments east of Florida. The variation of shear velocity and density with depth in such sediments was determined from Nafe and Drake (1957).

We may note that it is inconvenient to run such a model for each slight change in geology and water depth, especially when such a wide region is being considered as is the case here. Thus we have developed a short-hand method for determining Rayleigh wave velocities as a function of geology and bathymetry which for the range of velocities considered here, and for 5-s-period waves, gives consistently results about 90% of those obtained from the model. This was utilized to interpolate in areas with only minor changes and was continually compared with the more exact results. A discussion of this method is given in the appendix.

Having obtained the velocity at each location, we followed the procedure initially employed by Darbyshire (1955, 1963) and improved upon by Iyer et al. (1958) for Rayleigh waves approaching Bermuda, South Africa, and England, respectively. Wave fronts were drawn spreading from Palisades at 10-s time intervals. Orthogonals were then constructed radiating from Palisades perpendicular to the wave front at each point. By the principle of reciprocity these then also indicate the ray paths approaching Palisades. The velocity on the continent itself was set constant at 3.1 km/s. Although some variation would be expected for this frequency due to low-velocity sediments, the variation would not be great (Brune, 1969); the effect of topographic irregularities has been judged unimportant, to first order (Hudson and Knopoff 1967). The main concern here was the curvature of the ray paths approaching from oceanic sources.

Figure 3 presents the refraction diagram for microseisms of 5-s period at Palisades. The rays are drawn for every 2½° clockwise from 0° (due north) through 210°. In addition, we have included the grid lines and numbers from Figure 1 for comparison. In general, geometric spreading alone reduced the intensity of the incoming signal from distant regions, thereby qualitatively accounting for the low incidence of observed offshore sources. Several relative shadow zones appear, zones from which few rays propagate to Palisades. The most intense is along the southeast coast, in just the region (2) in which weak amplitudes and low incidence of microseismic sources are found as described previously. Refraction effects there appear to explain this observed anomaly. Also, it was noted by Blaik and Donn (1954) that when hurricanes moved from south to north a short distance off the east coast, approach directions usually remained to the southeast until the storm was well to the north of east; then they swung to the northeast also. This effect can also be quantitatively seen by noting the sparsity of rays due east offshore, in contrast to the rays from the northeast and especially the southeast. The refraction is greatest from the south and east because sediments (and thus velocity gradiations) are deposited essentially parallel to the coast, which trends southwest-northeast. For rays which are perpendicular to this axis, from the southeast, little refraction would be expected, while for rays at less of an angle, from the south and east, refraction is more effective. The great intensity of rays from the southeast, even off the continental shelf (represented by the dashed line) may account for the observation that the highest percentage of any microseism source region is found in this area (region 5). Thus the speculation that refraction effects could account for a number of observations involving microseisms has been shown to be correct.

Relation to Ocean Waves

We have discussed the location of the sources for microseisms recorded at Palisades and related the frequency of occurrence from specific locations to refraction effects. The next study concerns the relative strength of the microseisms recorded from sources in the different locations. To investigate this aspect, a comparison was made between the ocean waves in each suspected generating region and the average microseism amplitude for that hour as determined from the square root of the autocorrelation at zero phase lag. Linear regression relationships were determined between observed microseisms and both the ocean wave height (from computer printouts for the appropriate time) and the ocean wave height squared. The latter parameter is theoretically expected to be directly related to microseism pressure amplitude; however, a comparison of the two relationships indicates a slightly higher correlation between microseism amplitude and ocean wave height to the first power (0.55 as opposed to 0.5). The resulting microseism amplitudes predicted by the two methods for a given ocean wave height are within 5% of each other. Thus we will concentrate on the relationship between microseism amplitudes and ocean wave heights.

The hours chosen for analysis were the times (1) when microseisms showed only one seismic source (2) when the meteorological and oceanographic data indicated a well-defined single source clearly within a grid space (except for

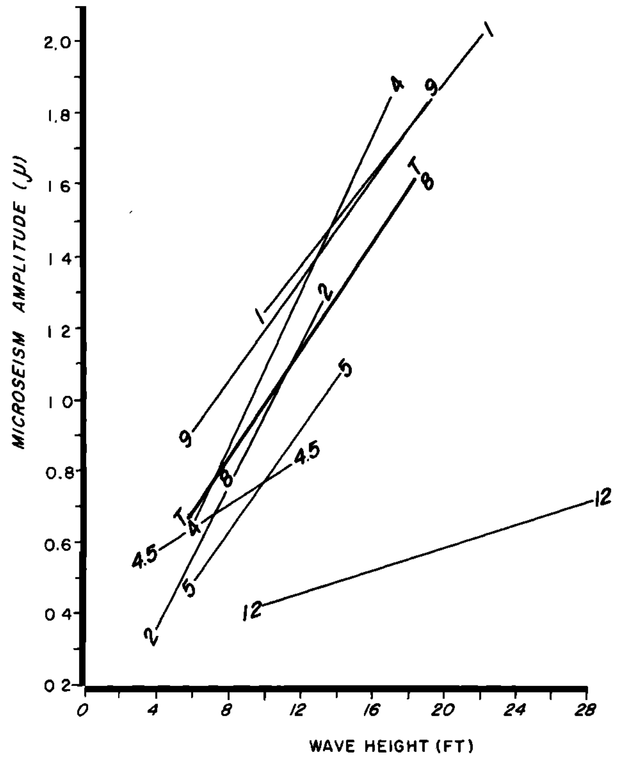

Fig. 4. Linear regression relationships between microseism ground motion in microns (μ) and ocean wave height in feet, for various source regions identified in Figure 1 and for the total (T) (266 hours).

sources which straddled regions 4 and 5) and (3) which were not within 12 hours of each other, to eliminate propagation time lag effects and correlation between observations. The resulting data sample was thus reduced to about one third of the total.

Figure 4 presents the regression relationships between the microseism ground amplitude recorded at Palisades and the ocean wave height in the suspected generating region identified by the numbers shown in Figure 1. The derived statistical parameters are given in Table 1. The results indicate that the relationship is statistically significant for each of the regions delineated. Thus microseism amplitudes from a particular station give a strong indication of ocean wave heights in a specific source region.

For each source region the line in Figure 4 is drawn from the mean value of the microseism amplitude plus or minus standard deviation. It can thus be seen that the largest amplitudes are received for ocean waves near the continental shelf and to the east or east-northeast of the station. Somewhat lower amplitudes are found for the same ocean wave heights for signals farther away to the northeast but still on the continental shelf (region 8). However, the region even further away and off the continental shelf (region 12) provides the lowest microseisms.

Regions to the south and southeast of Palisades provide lower-amplitude microseisms for the same height ocean waves. The region near shore (region 2) may have difficulty due to refraction effects, as discussed earlier, as may the region due east and partially off the continental shelf (regions 4 and 5). However, region 5, to the southeast, is definitely offshore with no refraction difficulties; the lower amplitudes observed on the coast thus appear to be from another cause, most likely due to a mode change from the fundamental to higher modes in crossing the ocean-continent boundary (e.g., McGarr, 1969), so that the energy is not confined to the surface and a lower surface wave amplitude results. This will be discussed further in the next article.

Microseisms with amplitudes greater than 3μ were not included in this study, as they generally resulted from several centers of high-amplitude ocean waves in the same vicinity. This observation has been noted previously (e.g., Dinger and Fisher, 1955; Geddes, 1958). The significance of ocean wave interaction will be discussed further in a later article. It should be noted that, as evidenced by the scatter listed in Table 1, it is impossible to predict ocean wave amplitude even in a particular region from microseisms observed at Palisades.

Summary and Conclusions

In this paper we have estimated the source locations of microseisms from analysis of the incoming wave particle motion using an analog correlator to compute the direction of propagation and then tracing this ray to a suspected meteorological-oceanographic source. We then determined the propagation path of Rayleigh waves approaching Lamont due to varying geological and bathymetric structure, and the resultant ray diagram was used to explain some of the observations of source-location frequency. Finally, we determined the amplitude of the observed microseisms as a function of ocean wave heights in the different locations and showed how the amplitudes were a function of refraction effects as well as apparently 'off the continental shelf' source locations. The principal conclusions of this study are as follows:

1. The majority of the sources producing microseisms at Palisades occur in regions either on the continental shelf to the east and northeast or off the continental shelf to the southeast, although the latter produce weaker signals for this continental station.

2. The apparent lower frequency of sources in the region along the southeast coast on the continental shelf appears to be due to refraction effects; rays leaving this zone do not arrive at Palisades.

TABLE 1. Statistics for Correlation Between Microseism Amplitudes Recorded at Palisades and Ocean Wave Height in Different Source Regions.

	Location	N*	b_{yx} †	a	S_{yx} ‡	r_{xy} "	Significance,¢ %
1	40°-45°N, 70°-75°W	36	0.065	0.588	0.47	0.698	1
2	30°-40°N, 70°-80°W	5	0.100	-0.43	0.29	0.834	5
4	40°-50°N, 60°-70°W	53	0.110	-0.007	0.74	0.622	1
5	30°-40°N, 60°-70°W	35	0.072	0.045	0.53	0.475	1
8	50°-60°N, 50°-60°W	49	0.076	0.209	0.75	0.443	1
9	40°-50°N, 50°-60°W	52	0.072	0.478	0.77	0.494	1
12	50°-60°N, 40°-50°W	6	0.016	0.265	0.08	0.862	1
4-5	35°-45°N, 60°-70°W	13	0.033	0.439	0.24	0.462	5
T	15°-80°N, 30°-160°W	266	0.076	0.232	0.68	0.547	1

*N is the number of hours.

† $Y = b_{yx}X+a$, where Y is the microseism amplitude in microns and X is the ocean wave height in feet (1 foot = 0.3 m).

‡ S_{yx} is the scatter in microns.

" r_{xy} is the correlation coefficient between microseism amplitude and ocean wave height.

¢ Significance (of r_{xy}) determined by F test, $F=(N-2)r^2/(1-r^2)$, with related statistical tables.

3. Microseism amplitude is correlated with ocean wave amplitude, but not to a great enough degree to allow one to be predicted by the other. In general, the closer the region is to the east or northeast on the continental shelf, the higher are the microseisms produced by given ocean waves. Sources farther away, or to our south, or off the continental shelf, produce lower amplitudes, due to geometric spreading of the energy, refraction effects, and possibly mode changes, respectively.

Appendix: Approximate Method of Determining Rayleigh Wave Velocity for a Given Geologic and Bathymetric Structure

An estimate of the Rayleigh wave velocity at each point can be obtained in the following manner: for each different layer, of known thickness and depth, the theoretical Rayleigh wave velocity was obtained from the observed compressional wave velocity (the Poisson ratio for depths of interest is close to 0.25). The Rayleigh velocity, as a function of the ground structure alone, was calculated from the formula

$$V_R = \frac{\sum_{i=1}^{n} V_i Z_i e^{-\gamma_a Z_{im}}}{\sum_{i=1}^{n} Z_i e^{-\gamma_a Z_{im}}}$$

where V_i is the Rayleigh velocity, Z_i is the thicknesses for each layer down to 7.5-km depth below the sea floor, and Z_{im} is the mean depth of the layer. Here $\gamma_a = \frac{\gamma+\gamma^1}{2}$ with $\gamma^2=K^2-\omega^2/\alpha^2$ and $(\gamma^1)^2=K^2-\omega^2/\beta^2$. The exponential term thus reproduces the falloff of influence of deeper layers on the velocity in the same way that the amplitude of the surface wave decreases with depth. The other terms in the numerator incorporate the influence of the different velocities and thicknesses. The denominator provides the normalization for the depth function. Although the term γ_a should truly be an iterative result, as it depends on the wave number K, which is itself a function of the phase velocity, the value used throughout is $\gamma_a = 0.30$, which is appropriate for a phase velocity of 3.5 km/s. The variation of this parameter for the range of velocities derived does not alter the results significantly considering the other uncertainties. The justification for limiting the velocity dependence on the ground structure down to 7.5 km rests on the calculation that for an ideal Rayleigh wave with the above velocity the amplitude is reduced to 10% of its surface value at this depth. For lower velocities and thus shorter wavelength there is even less reason to consider deeper levels.

To incorporate the influence of varying ocean depth, the ground structure at each location was considered to be homogeneous with the previously calculated velocity, overlain by water of the given thickness. The final velocity was interpolated for these two parameters from various phase velocity curves for liquid layers over different solid substances, assuming the lowest-order mode (M. Ewing et al., 1957). The results agreed with observations for waves of this frequency previously observed at Lamont (Oliver, 1962).

The velocities estimated by this type of calculation were compared to the exact values obtained from the model described earlier. The estimated velocity was consistently about 90% of the more exact determination.

Acknowledgments. We would like to thank Henry Kutschale for his help in utilizing computer programs. This work was indirectly supported by National Science Foundation contract ATM 09449 and U.S. Army Research DAAG 29-77-G-0131. Lamont-Doherty Geological Observatory contribution #2668.

References

Blaik, M., and W. L. Donn, Microseism ground motion at Palisades and Weston, Bull. Seismol. Soc. Amer., 44, 597-612, 1954.

Bradner, H., L. de Jerphanion, and R. Langlois, Ocean microseism measurements with a neutral buoyancy free-floating midwater seismometer, Bull. Seismol. Soc. Amer., 60, 1139-1150, 1970.

Brune, J. N., Surface waves and crustal structure, in The Earth's Crust and Upper Mantle, Geophys. Monogr. Ser., Vol. 13, edited by P. J. Hart, AGU, Washington, D. C., 1969.

Darbyshire, J., Refraction of microseisms at island stations, Mon. Notic. Roy. Astron. Soc., 7, 1473, 1955.

Darbyshire, J., A study of microseisms in South Africa, Geophys. J. Roy. Astron. Soc., 8, 165-175, 1963.

Dinger, J., and G. Fisher, Microseism and ocean wave studies on Guam, Eos Trans. AGU, 36, 262-272, 1955.

Donn, W. L., Direction studies using microseism ground-particle motion, Eos Trans. AGU, 35, 821-832, 1954.

Donn, W. L., A case study bearing on the origin and propagation of 2- to 6- s microseisms, Eos Trans. AGU, 38, 354-359, 1957.

Drake, C., N. Campbell, G. Sander, and J. Nafe, A mid-Labrador sea ridge, Nature, 200, 1085-1086, 1963.

Ewing, J., and M. Ewing, Seismic-refraction measurements in the Atlantic Ocean basins, in the Mediterranean Sea, on the Mid-Atlantic Ridge, and in the Norwegian Sea, Geol. Soc. Amer. Bull., 70, 291-318, 1959.

Ewing, M., W. Jardetsky, and F. Press, Elastic waves in layered media, McGraw-Hill, New York, 1957.

Fenwick, D., M. Keen, C. Keen and A. Lambert, Geophysical studies of the continental margin northeast of Newfoundland, Can. J. Earth Sci., 5, 483, 1968.

Geddes, A., A survey of the microseisms recorded at Aberdeen in 1955, together with a review of the meteorological conditions under which they may have arisen, Bull. Seismol. Soc. Amer., 48, 65-76, 1958.

Haubrich, R., Earth noise, 5 to 500 millicycles per second, 1, Spectral stationarity, normality, and nonlinearity, J. Geophys. Res., 70, 1410-1427, 1965.

Haubrich, R., and K. McCamy, Microseisms: Coastal and pelagic sources, Rev. Geophys. 7, 539-572, 1969.

Haubrich, R., W. Munk, and F. Snodgrass, Comparative spectra of microseisms and swell, Bull. Seismol. Soc. Amer., 53, 27-37, 1963.

Heezen, B., M. Tharp, and M. Ewing, The floors of the oceans, 1, The North Atlantic, Geol. Soc. Am. Spec. Pap. 65, 1959.

Houtz, R., and J. Ewing, Detailed sedimentary velocities from seismic refraction profiles in the western North Atlantic, J. Geophys. Res., 68, 5233-5258, 1963.

Hudson, J., and L. Knopoff, Statistical properties of Rayleigh waves due to scattering by topography, Bull. Seismol. Soc. Amer., 57, 83-90, 1967.

Ikegami, R., An observational study on the propagation of microseismic waves, Bull. Tokyo Gakugei Univ., 13, 197-209, 1962.

Ikegame, R., and F. Kishinouye, A study on the propagation of microseismic waves, V, Bull. Earthquake Res. Inst. Tokyo Univ., 29, 571-576, 1951.

Iyer, H., A study on the direction of arrival of microseisms, at Kew Observatory, Geophys. J. Roy. Astron. Soc., 1, 32-43, 1958.

Iyer, H., D. Lambeth, and B. Hinde, Refraction of microseisms, Nature, 191, 646-647, 1958.

Kutschale, H. W., The integral solution of the sound field in a multilayered liquid-solid half-space with numerical computations for low-frequency propagation in the Arctic Ocean, Tech. Rep. 1, Columbia Univ., Palisades, N. Y., 1970.

Kutschale, H. W., Further investigation of the integral solution of the sound field in multilayered media; A liquid-solid half space with a solid bottom, Tech. Rep. 6, Columbia Univ., Palisades, N. Y., 1971.

Latham, G., and G. Sutton, Seismic measurements on the ocean floor, J. Geophys. Res., 71, 2545-2573, 1966.

Le Pichon, X. L., R. Hyndman, and G. Pautot, Geophysical study of the opening of the Labrador Sea, J. Geophys. Res., 76, 4724-4743, 1971.

McGarr, A., Amplitude variations of Rayleigh waves-propagation across a continental margin, Bull. Seismol. Soc. Amer., 59, 1281-1305, 1969.

Monakhov, F., Microseisms at the bottom of the Baltic Sea and in the northern part of the Atlantic Ocean, Bull. Acad. Sci. USSR Geophys. Ser., 12, 573-580, 1962.

Nafe, J., and C. Drake, Variation with depth in shallow and deep water marine sediments of porosity, density and the velocities of compressional and shear waves, Geophysics, 22(3), 523-552, 1957.

Nafe, J., and C. Drake, Floor of the North Atlantic-Summary of geophysical data, North Atlantic-Geology and Continental Drift, Amer. Ass. Petrol. Geol. Mem. 12, 59-87, 1969.

Oliver, J., A summary of observed seismic surface wave dispersion, Bull. Seismol. Soc. Amer., 52, 81-86, 1962.

Rygg, E., H. Bungun, and L. Bruland, Spectral analysis and statistical properties of microseisms at NORSAR, Sci. Rep. 1, Seismol. Observ., Univ. of Bergen, Bergen, Norway, 1969.

Sheridan, R., and C. Drake, Seaward extension of the Canadian Appalachians, Can. J. Earth. Sci., 5, 337-373, 1968.

Sheridan, R., C. Drake, J. Nafe, and J. Hennion, Seismic-refraction study of continental margin east of Florida, Amer. Ass. Petrol. Geol. Bull., 59, (9), 1972-1991, 1966.

(Received September 22, 1977;
revised December 20, 1977;
accepted March 15, 1978.)